Atmos. Meas. Tech., 4, 2441–2451, 2011
www.atmos-meas-tech.net/4/2441/2011/
doi:10.5194/amt-4-2441-2011

Atmospheric Measurement Techniques

Improving measurements of SF_6 for the study of atmospheric transport and emissions

B. D. Hall[1], G. S. Dutton[2], D. J. Mondeel[2], J. D. Nance[2], M. Rigby[3], J. H. Butler[1], F. L. Moore[2], D. F. Hurst[2], and J. W. Elkins[1]

[1]NOAA Earth System Research Laboratory, Boulder, CO 80305, USA
[2]Cooperative Institute for Research in Environmental Sciences, University of Colorado, Boulder, CO 80309, USA
[3]Center for Global Change Science, Massachusetts Institute of Technology, 77 Massachusetts Ave., Cambridge, 02139 MA, USA

Received: 9 June 2011 – Published in Atmos. Meas. Tech. Discuss.: 4 July 2011
Revised: 20 October 2011 – Accepted: 25 October 2011 – Published: 14 November 2011

Abstract. Sulfur hexafluoride (SF_6) is a potent greenhouse gas and useful atmospheric tracer. Measurements of SF_6 on global and regional scales are necessary to estimate emissions and to verify or examine the performance of atmospheric transport models. Typical precision for common gas chromatographic methods with electron capture detection (GC-ECD) is 1–2 %. We have modified a common GC-ECD method to achieve measurement precision of 0.5 % or better. Global mean SF_6 measurements were used to examine changes in the growth rate of SF_6 and corresponding SF_6 emissions. Global emissions and mixing ratios from 2000–2008 are consistent with recently published work. More recent observations show a 10 % decline in SF_6 emissions in 2008–2009, which seems to coincide with a decrease in world economic output. This decline was short-lived, as the global SF_6 growth rate has recently increased to near its 2007–2008 maximum value of 0.30 ± 0.03 pmol mol^{-1} (ppt) yr^{-1} (95 % C.L.).

1 Introduction

Sulfur hexafluoride (SF_6) is a potent greenhouse gas with a global warming potential (100 yr time horizon) 22 800 times that of carbon dioxide (Forster et al., 2007). Because of its very long lifetime (800–3200 yr) (Ravishankara, et al., 1993; Morris et al., 1995) and the fact that the only known sink is destruction in the mesosphere, the atmospheric burden is essentially equal to the total amount of SF_6 emitted during the industrial era. While some voluntary efforts to reduce the amount of SF_6 emitted to the atmosphere have been made (Harnisch and Gluckman, 2001; US EPA, 2008) the atmospheric concentration continues to rise (Elkins and Dutton, 2009; Levin et al., 2010; Rigby et al., 2010). Efforts to quantify SF_6 emissions have been performed using bottom-up inventories and top-down methods based on atmospheric concentration and variability (UNFCCC, 2010; Maiss and Brenninkmeijer, 1998; Bakwin et al., 1997; Hurst et al., 2007; Levin et al., 2010; Rigby et al., 2010). Reconciling discrepancies between top-down and bottom-up emissions should, in principle, be relatively simple compared to other greenhouse gases for which there are natural sources or sinks that are more difficult to quantify (eg. N_2O and CH_4). Still, discrepancies between bottom-up and top-down emissions estimates of SF_6 remain (Levin et al., 2010), and estimating emissions on regional scales by top-down methods remains challenging (Rigby et al., 2010). Measurement precision is one of the limiting factors in estimating emissions through atmospheric inversion methods (Rigby et al., 2010).

Measurements of atmospheric SF_6 obtained by a number of researchers around the world are used to examine trends in SF_6 emissions (Levin et al., 2010; Rigby et al., 2010), evaluate atmospheric transport models (Levin and Hesshaimer, 1996; Gloor et al., 2007; Patra et al., 2009), and for the study of stratospheric circulation and the calculation of air mass mean age (Park et al., 1999, Engel et al., 2008, Ray et al., 2010). The predominant method of SF_6 measurement involves gas chromatography with detection by electron capture detector (ECD) or mass selective detector (MSD). Although pre-concentration has been used

Correspondence to: B. D. Hall
(bradley.hall@noaa.gov)

(Wanninkhof, 1991; Miller et al, 2008), the ECD is sufficiently sensitive to SF_6 that pre-concentration is generally not required. With the ECD, SF_6 is typically separated from other ECD-sensitive gases using packed columns, such as molecular sieve 5A (Simmonds et al., 1972) or Porapak-Q (Elkins, 1980; Elkins et al., 1996; Hall et al., 2007); Because nitrous oxide (N_2O) and SF_6 can both be resolved using Porapak-Q (or Hayesep-Q) columns, this method is commonly employed (Worthy et al., 2003; van der Laan et al., 2009; Thompson et al., 2009). Hayesep-Q and Porapak-Q are similar in their characteristics and result in similar chromatography. Typical precision for most ambient SF_6 measurements using ECDs is 1–2 %. Better precision can sometimes be achieved using pre-concentration, but this adds additional complexity, and is not as common as loop-injection air samples.

Here we describe GC systems used to perform SF_6 calibrations since 1999. We first describe a Porapak-Q-based system similar to that used to measure SF_6 in NOAA/ESRL flask samples of ambient air since 1995 (Geller et al., 1997). Then we describe how this method was modified to improve SF_6 precision on a laboratory-based GC used for calibration, and also on one in situ system. Finally, we use global and hemispheric mean SF_6 from NOAA/ESRL flask and in situ networks to examine recent changes in emissions of SF_6.

The main advantage to the method described here is that it involves a relatively simple conversion of a GC method commonly used for N_2O and SF_6 measurement that improves SF_6 without compromising N_2O. While laser-based N_2O instruments are emerging, gas chromatography with electron capture detection is commonly used for SF_6, and GC-ECD systems measuring both N_2O and SF_6 will likely be used for the foreseeable future.

2 Methods

The chromatography often associated with the measurement of SF_6 is basically the same as that used to measure N_2O (Elkins 1980; Elkins et al., 1996; Hall et al., 2007). Typically, a 10-port or 12-port, 2-position gas sample valve (GSV) is used to direct an air sample through two columns and an ECD. With calibration and in situ systems we currently use a 12-port GSV (Valco Instrument Co., Houston, TX) operated in "heart cut" mode to prevent the majority of the oxygen/nitrogen in the sample from reaching the ECD (Fig. 1). Upon injection, the sample is directed onto the pre-column. When the gases of interest reach the main column, the GSV is switched (Table 1), directing flow from the main column to the ECD, while flow through the pre-column is reversed (backflushed) to prevent unwanted compounds from accumulating on the main column. A pressure perturbation results in a slight baseline change, followed by the elution of N_2O and SF_6 (Fig. 2a). The SF_6 precision, defined as one standard deviation of a series of 8–10 determinations of SF_6 concentration, is typically 1–2 %. Changes in ECD response (drift) are monitored by alternating the unknown with injections of a natural-air working standard. Both 5 % Ar in CH_4 (P-5) and nitrogen with dynamic CO_2 doping have been used with similar SF_6 precision (Moore et al., 2003; Hall et al., 2007). Table 1 shows the evolution of dedicated calibration instruments from 1999 to present.

In 2006 we were using an Agilent ECD (G1533A) with two Porapak-Q columns and CO_2-doped N_2 carrier gas (Hall et al., 2007; version 2 in Table 1). This system was modified in June 2006 by adding a third column (post-column). The three-column method was first described by Moore et al. (2003), who used this method for balloon-borne measurements of N_2O and SF_6 at 70 s resolution. The objective of Moore et al. (2003) was to improve the temporal resolution of N_2O and SF_6 by speeding up the chromatography. The work described here was done specifically to improve SF_6 precision without compromising N_2O. While conceptually similar, motivation and optimization of the two systems differed.

The change to the three-column system involved decreasing the lengths of the Porapak-Q columns and adding a post-column (molecular sieve 5A, 185 °C) to the end of the Porapak-Q main column. The effective "main" column thus consists of a Porapak-Q column in series with a MS-5A column, operating at different temperatures. The MS-5A column was installed in a custom-built heated zone, controlled with an Omega (Omega Engineering, Stamford, CT) temperature controller (185 ± 0.1 °C). The temperature of the Porapak-Q columns (both pre and main) was increased from 56 °C to 90 °C. In this way, the Porapak-Q columns are used only to separate N_2O and SF_6 from "air". N_2O and SF_6 elute from the Porapak-Q columns at nearly the same time and are separated from each other on the MS- 5A column. Because N_2O is more retentive than SF_6 on MS-5A the order of elution is reversed compared to using Porapak-Q alone (Fig. 2). SF_6 elutes earlier in the chromatogram, resulting in a gain in peak height without an increase in noise. During the modification period, MS-5A 80/100 mesh was tried. However, the higher mesh was too restrictive and was abandoned in favor of 40/60 mesh. We also experimented with different lengths of MS-5A column, and different Porapak-Q temperatures. A balance must be reached in which the N_2O and SF_6 are sufficiently separated from oxygen (air) but not separated from each other as they enter the post-column. If the Porapak-Q columns are too cool, N_2O and SF_6 will separate in the wrong order and then must be re-separated on the MS-5A column. There is also a potential drawback in operating the Porapak-Q columns at too high of a temperature as the porous polymer could be oxidized in the presence of oxygen. Our system has been operating at 90 °C since 2006 and we have not observed evidence of degradation.

Once the new columns were installed, we used a thermal conductivity meter to detect the air peak eluting from the MS-5A column while in "inject" mode (in which the air peak is vented). Identifying the timing of the air peak helps to set

Table 1. Configuration of three SF_6 GCs used for calibration since 1999.

	Version 1	Version 2	Version 3
Period of use	Sep 1999–Feb 2003	Feb 2003–Jun 2006	Jul 2006–present
Pre-column	2m × 3.7 mmI.D., 4.76 mm O.D. Porapak-Q, 80/100 mesh	2m × 3.7 mm I.D., 4.76 mm O.D. Porapak-Q, 80/100 mesh	1m × 3.7 mm I.D., 4.76 mm O.D. Porapak-Q, 80/100 mesh
Main column	3 m × 3.7 mm I.D., 4.76 mm O.D. Porapak-Q, 80/100 mesh	3 m × 3.7 mm I.D., 4.76 mm O.D. Porapak-Q, 80/100 mesh	2 m × 3.7 mm I.D., 4.76 mm O.D. Porapak-Q, 80/100 mesh
Post-column	NA	NA	0.91 m × 3.18 mm O.D. O.D. sieve mol.5A 40/60 mesh
Pre-column T (°C)	55	56	90
Main-column T (°C)	55	56	90
Post-column T (°C)	NA	NA	185
Flow control	MFC	MFC/EPC	EPC
Detector	Valco (140BN)	Agilent (G1533A)	Agilent (G1533A)
Carrier gas	5 % CH_4/Ar (P-5)	N_2 (w/CO_2 doping)	N_2 (w/CO_2 doping)
CO_2 at ECD outlet (ppm)	NA	∼1650	∼2500
SF_6 retention time (s)	∼440	515–545	305
SF_6 peak width (s)	∼24	30	23
N_2O retention time (s)	∼345	405–435	410
N_2O peak width (s)	∼18.5	23	27
ECD T (°C)	350	340	340/370
Run time (s)	1800	900	720
GSV switch (s)	240	300–320	180
CO_2 retention time (s)	∼270	∼365	∼475

T: temperature; MFC: mass flow controller; EPC: electronic pressure controller.

the timing of the GSV switch. With a main carrier gas flow rate of 31 sccm, the air peak was observed at 125 s. We then performed several injections to optimize the valve timing. At switch times between 170 and 195 s, N_2O and SF_6 remained constant. A switch time of 180 s was chosen, which resulted in retention times of 305 and 410 s for SF_6 and N_2O respectively. The lengths of our Porapak-Q columns were chosen as a matter of convenience (i.e. already available). Other combinations may also be suitable.

Following the column changes, the CO_2 doping level was adjusted for optimal N_2O response. High-purity CO_2 is added through a crimped tube (10 cm × 1.58 mm O.D., 0.127 mm I.D.) and enters the flow stream prior to the ECD. The CO_2 flow rate (∼0.08 cc min^{-1}) is controlled through a constant head pressure on the crimp. The N_2O and SF_6 responses were tested at different CO_2 pressure settings. The N_2O response showed a maximum at about 124 kPa, which corresponds to 2500 ppm CO_2 in the ECD. The SF_6 response declined with increasing CO_2 (Fig. 3).

One potential drawback with this technique is that CO_2 may co-elute with N_2O, depending on the operating temperature of the MS-5A column. In the present case, CO_2 elutes under the tail of the N_2O peak (Fig. 2b). All of our systems that employ the 3-column method also employ N_2 carrier gas with CO_2 doping. Thus, the amount of CO_2 present in the detector is only slightly perturbed as the sample CO_2 elutes. It is desirable to set the CO_2 concentration such that the N_2O response is insensitive to small changes in CO_2, i.e. not affected by varying amounts of CO_2 in the sample or by small changes in the pressure of the dopant delivery system. At 2500 ppm CO_2, the sensitivity to ± 10 ppm fluctuations in CO_2 dopant is a factor of 10 less than the typical 1-σ precision for both N_2O and SF_6. Insensitivity to sample CO_2 was further verified by comparing air samples with and without CO_2 (CO_2 was completely removed using sodium hydroxide-coated silica – Ascarite). The response ratios for samples with and without CO_2 was 0.99964 ± 0.00033 for N_2O and 0.9998 ± 0.0046 for SF_6, which translates into biases of 0.1 ppb and 0.001 ppt, respectively, and is insignificant considering the much smaller natural variations of CO_2 in the atmosphere.

The use of CO_2 doping may also minimize interference between N_2O and CO that might be produced from Porapak. Any CO produced would likely react on hot metal surfaces to form CO_2 (Fehsenfeld et al., 1981), which could interfere with N_2O if not for the excess CO_2 supplied by doping. We have not determined if column-generated CO interferes with N_2O when using P-5 carrier gas.

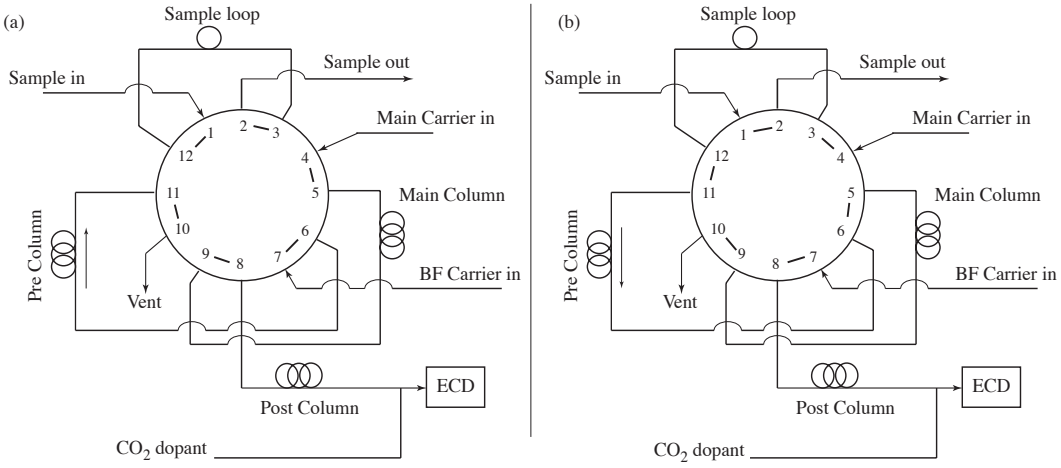

Fig. 1. Diagram of 12-port gas sample valve (GSV) in **(a)** load, and **(b)** inject modes. Note that Air (O_2/N_2) is vented during inject mode, and the sample is directed from the main and post columns to the ECD in load mode.

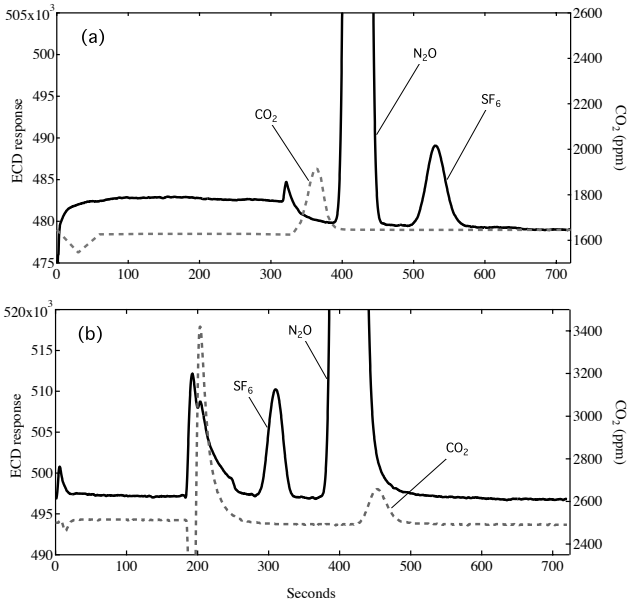

Fig. 2. Sample chromatograms from two-column N_2O/SF_6 analysis system (upper panel, version 2) and three-column system (lower panel, version 3) (see Table 1). CO_2 was measured at the outlet of the ECD.

Prior to installing the post-column, mass flow controllers were replaced with electronic pressure controllers (EPC), and used to set the head pressures on the main and pre-columns. This was done to reduce the effects of changes in room pressure on flow rates. The EPCs are less sensitive to changes in ambient pressure, possibly because they control pressure relative to a reference pressure (ambient pressure in this case) and thus maintain a constant ΔP relative to the ECD outlet.

3 Results

3.1 Calibration instruments

With the three-column system, the SF_6 precision was improved from 1–2 % to better than 0.5 %. SF_6 precision determined from analysis of various gas standards is shown in Fig. 4. The signal to noise (calculated as SF_6 peak height of a 5.8 ppt sample relative to the standard deviation of the ECD baseline under stable conditions) improved from ∼115 to ∼160 following the addition of the post-column. The SF_6 peak height increased by 37 % while the baseline noise remained unchanged. The mean precision for 5-month periods before and after the addition of the post-column (from 40 ambient-level samples in each period) was 0.72 (std. dev. 0.24) % and 0.45 (0.13) %, respectively. Prior to the addition of the post-column precision was variable, and seemed to show some improvement in late 2005 resulting from a change in the crimp used to control CO_2 dopant flow. The change from mass flow controllers to electronic pressure controllers (early 2006) may have also helped, but the largest improvement corresponds with the addition of the MS-5A post-column in mid-2006 (Fig. 4, lower panel). The change in flow controllers did not result in decreased variability of the SF_6 retention time. In fact, a significant reduction in retention time variability occurred following the addition of the post column ($\sigma = 0.18$ s with EPC and two columns, $\sigma = 0.10$ s with EPC and three columns) rather than with the installation of the EPC. Further, a change in flow controllers (from custom-built MFC to commercial MFC, Pnucleus Tecnologies, Hollis, NH) on two separate systems using only Porapak-Q columns (installed at South Pole and Summit, Greenland) made little difference to the SF_6 precision.

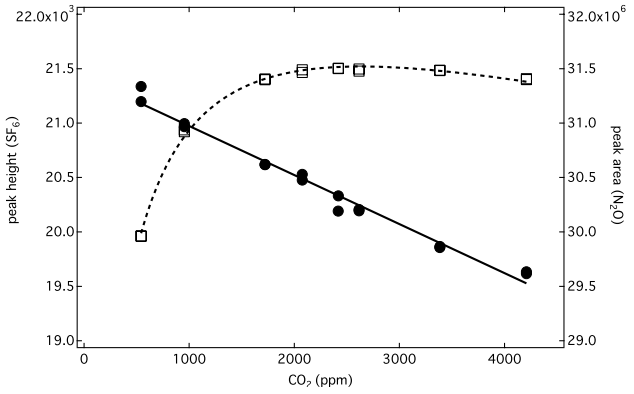

Fig. 3. Effect of CO_2 on SF_6 (left axis, closed circles) and N_2O (right axis, open squares) response (arbitrary units).

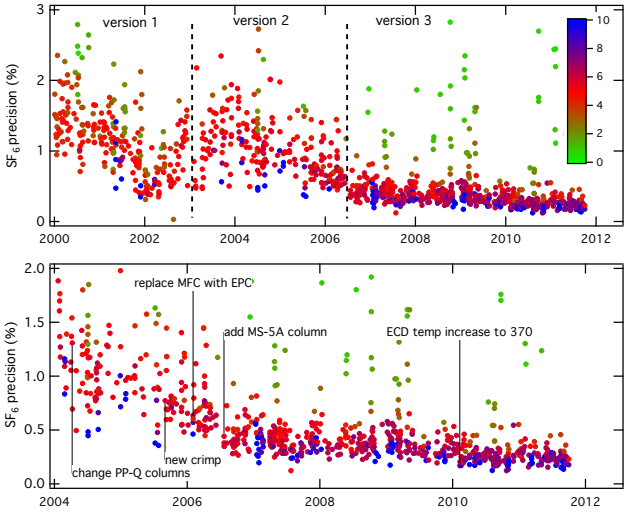

Fig. 4. History of SF_6 precision (%) from all samples analyzed on the GC-ECD systems used for calibrations (color-coded by SF_6 mole fraction – ppt). Upper plot shows three GC versions. Lower plot shows versions 2 and 3 along with system changes.

A substantial benefit is that the current system has been essentially maintenance-free over the last four years. SF_6 retention time, peak width, and peak response have remained very stable since the modifications were made. Compared to our original system (Version 1), the use of N_2 carrier gas has eliminated some of the variability caused by variations in P-5 quality. High-purity nitrogen is more easily obtained, and the quality of N_2 is more consistent than that of P-5, which can sometimes contain significant amounts of SF_6 (Elkins et al., 1996).

The improvements in precision and stability have allowed us to develop an improved reference scale for SF_6 based on standards prepared by gravimetric methods. Nine compressed gas standards were prepared between 2003 and 2005 as described in Hall et al. (2007). These were combined with seven standards prepared in 2000 to establish the NOAA-2006 SF_6 calibration scale (adopted by WMO/GAW) over the range 1–10 ppt (dry air mole fraction) (Table 2) (see also http://www.esrl.noaa.gov/gmd/ccl/sf6_scale.html). The NOAA-2006 scale compares within 0.01 ppt with the Scripps Institution of Oceanography (SIO-05) (Rigby et al., 2010) and within 0.03 ppt of the University of Heidelberg Scale (Hall et al., 2011).

With GC version 3, the standards were analyzed several times relative to a natural-air working standard. The response was linear and a fit of the relative response (peak height) showed a zero intercept. Although a zero intercept was expected from previous work, we were not able to confirm this until the improved precision was realized with GC version 3. This important feature means that calibrations can be carried out by ratio to a single working standard as long as the response remains linear. We are exploring the range over which linearity can be assumed; currently 1–10 ppt. Reproducibility (1-σ) of SF_6 assignments has improved from 0.05-0.07 ppt using GC version 1, to 0.03–0.05 ppt using GC version 2, and finally to $<= 0.02$ ppt using GC version 3.

Five secondary natural air standards (3–11 ppt) are used to verify the instrument response function (calibration run) every other month. The SF_6 response function is stable enough that more frequent calibration is not necessary. This was not true of GC version 1. Secondary standards were assigned values on the NOAA-2006 scale. Using the five secondary standards to predict the value of the working standard during each calibration run (linear model (a): $Y = aX$), we find that the predicted value of the working standard has varied by no more than 0.011 ppt over a three-year period. The standard deviation of predicted values is 0.003 ppt. Similar results were achieved linear model (b): $Y = aX + b$. In this case the range of predicted values varied by no more than 0.013 ppt and the standard deviation of all predictions was 0.004 ppt.

Regular analysis of other natural air standards also shows improved precision and stability (Fig. 5). The reproducibility of SF_6 assignments is particularly good following the 2006 modifications. Standard deviations of a "target" standard analyzed between mid-2006 and 2009 are 0.012 and 0.014 ppt using linear models (a) and (b) respectively. Other secondary standards show similar precision on repeated analysis. The long-term precision is comparable to the short-term precision, indicating that there are no significant long-term variations that would lead to a time-dependent bias. Regulator effects might be one reason why SF_6 measurement precision is better for the working standard (blue symbols in Figs. 4 and 5) compared to the target cylinders. We have noticed that some regulators seem to perform better than others, even among the same model number. While long-term conditioning to the air stream (i.e. dedicated regulators) may help in some cases, it does not always lead to improvements.

We have performed limited testing of the current configuration (version 3 in Table 1) with an Agilent μ-ECD

Table 2. Standards that define the NOAA-2006 SF_6 calibration scale.

Cylinder	Year	Prepared (ppt)	Assigned (ppt)	Residual (ppt)
FA-1861	2000	2.41	2.39	−0.02
FA-1878	2000	2.91	2.89	−0.02
FA-1843	2000	4.73	4.76	0.03
FA-1850	2000	4.51	4.53	0.02
FA-1851	2000	4.32	4.35	0.02
FA-1856	2000	1.14	1.15	0.01
FA-1865	2000	4.12	4.13	0.01
FA-2205	2000	4.94	4.92	−0.02
FA-2207	2003	5.98	5.98	0.00
FA-2208	2003	6.97	7.01	0.03
FA-1940	2005	1.52	1.49	−0.03
FA-2139	2005	3.13	3.14	0.01
FA-2557	2005	3.86	3.85	−0.01
FA-2567	2005	5.99	6.02	0.03
FA-2569	2005	7.92	7.90	−0.02
FA-2585	2005	9.83	9.79	−0.04

(G2397A). An Agilent μ-ECD was installed in the calibration GC and the column outlet was simply moved from one detector to the other while all operating conditions remained the same. The smaller internal volume of the μ-ECD results in peaks with slightly smaller peak width (see Supplement Fig. S1). While the optimal CO_2 dopant concentration is lower with the Agilent μ-ECD (500–700 ppm) (A. Crotwell, personal communication, 2010) compared to the Agilent ECD (∼2500 ppm), precision, peak shape, and baseline behavior are similar. While we have not used this technique with a μ-ECD for extended periods of time, limited testing suggest that this technique is fully compatible with the μ-ECD.

3.2 In situ instrument

We have also performed modifications similar to those described above to an in situ N_2O and SF_6 measurement system installed at a mountain site (Niwot Ridge) in Colorado. The original GC configuration was similar to version 1 (Valco ECD), but is now operated with a MS-5A post-column and CO_2-doped N_2 carrier gas similar to version 3. Figure 6 shows hourly data from this site for selected periods in 2006 and 2009. SF_6 precision during periods without obvious pollution events was ∼2 % in 2006 and <0.5 % in 2009, a factor of four improvement. Small pollution events can be seen in Fig. 6b, which would have gone undetected earlier.

In addition to the post-column, mass flow controllers used to control carrier gas flows and electrical connections to the ECD were replaced. The improvement in SF_6 precision is due to a combination of these modifications, which were performed simultaneously. We do not know exactly how much the addition of the post-column contributed to the improved precision on this instrument. Similar changes to the MFCs on two other systems had little effect.

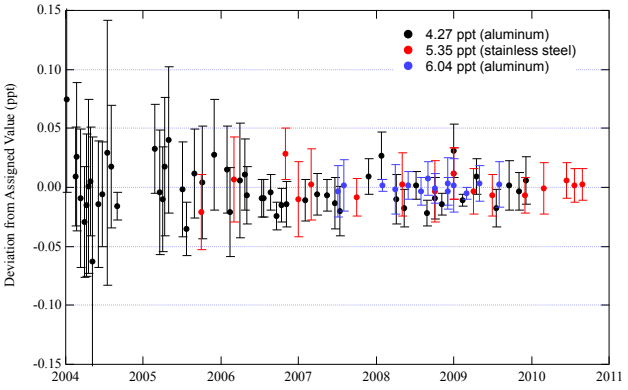

Fig. 5. Reproducibility of SF_6 calibration assignments. Since 2006 the mean deviation has been −0.005 ppt, 0.002, and 0.005 ppt for 4.27, 5.35, and 6.04 ppt target standards, respectively.

3.3 A history of atmospheric SF_6

A history of global atmospheric SF_6 was compiled from a combination of grab samples (flasks) and in situ measurements obtained by the NOAA/ESRL halocarbons group at multiple sites dating to 1995. A history based on two observing programs (one based on flasks and the other in situ) was developed by combining flask and in situ results into a single integrated record at each observing site. Both flask and in situ records offer different advantages and dis-advantages. Flask observations yield greater spatial coverage with lower temporal resolution. Flasks are analyzed on a single laboratory instrument, which should, in principle, be subject to fewer calibration and operational issues than instruments located at remote sites. However, because a single instrument is used, instrument malfunction or performance would affect all flasks analyzed during that period. In situ observations offer greater temporal resolution but lower spatial coverage compared to flasks. Calibration transfer issues would likely be averaged out over time since each in situ instrument is calibrated independently. Flask and in situ instruments are calibrated using two natural-air working standards (one at near-ambient level, and one diluted by 10 % with SF_6-free air) to account for non-linearity. These standards are traceable to the NOAA-2006 scale via the primary calibration GC (described above) and are replaced about every 2 yr. A 10 % concentration difference is generally sufficient to establish the SF_6 response curve (assumed linear over this range) because these instruments are located in remote places where SF_6 concentrations seldom exceed that of the highest working standard by more than 20 %. We have observed a slight non-linear behavior of the ECD in the calibration instrument, but errors are less than 0.03 ppt at concentrations within 30 % of the working standard.

Figure 7 shows global and hemispheric mean SF_6 from 1995 to present from the integrated SF_6 record. SF_6 data from six in situ sites (BRW, SUM, NWR, MLO, SMO, SPO)

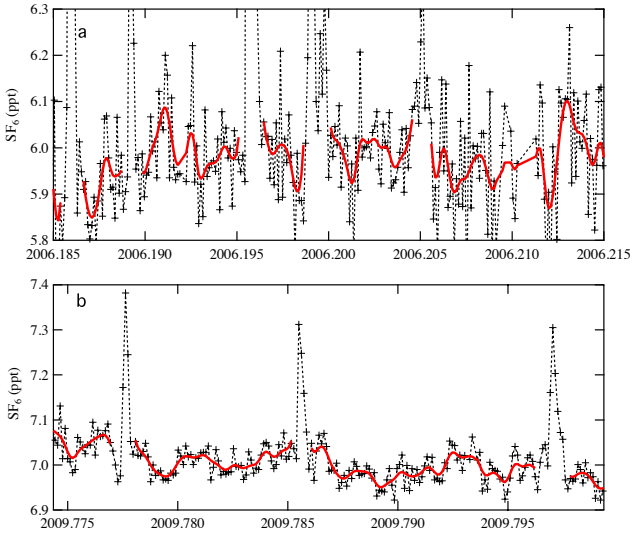

Fig. 6. Time series of SF_6 at Niwot Ridge, Colorado showing baseline conditions and pollution events during two periods: **(a)** prior to GC modification; **(b)** following GC modification. Both panels show a smooth fit to baseline data (approximate) (red lines).

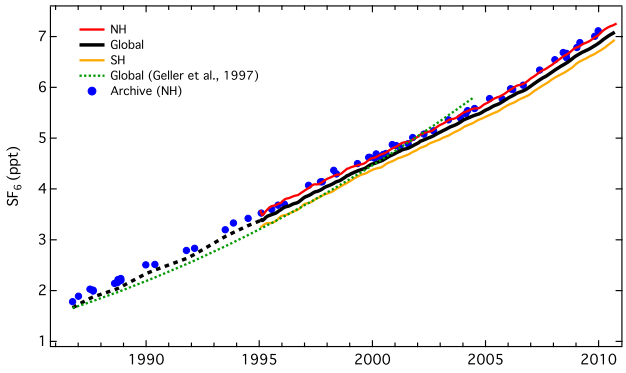

Fig. 7. Global and hemispheric mean SF_6 from flask and in situ data along with NH archive samples. The dashed line prior to 1995 represents the global mean derived from NH archive data (computed from a lowess fit to the NH archive record minus the mean difference (0.14 ppt) between NWR and the global mean from 1995–2005). A linear fit of global mean SF_6 as a function of time (t) from 1986–2005 yields: $y = 1.25(0.01) + 0.215(0.001) \times (t–1985)$.

were merged with flask data from twelve sites (ALT, SUM, BRW, MHD, NWR, THD, MLO, KUM, SMO, CGO, PSA, SPO) (see Table 3, Supplement Fig. S2). At sites in which both flask and in situ data exist, monthly mean (flask) and median (in situ) were averaged together weighted by standard deviation. Data gaps (typically only a few months) were filled using linear interpolation. Monthly median in situ data were used instead of monthly mean in order to minimize the effects of local influence in the in situ records. Flasks are normally collected under background conditions. In most cases 3–5 flasks pairs per month were combined with ∼400–700 hourly in situ samples (data source:http://www.esrl.noaa.gov/gmd/hats/combined/SF6.html).

The history was extended to the mid-1980's by analyzing cylinders of air collected at Niwot Ridge, Colorado. The archive consists mostly of 29.5-l aluminum cylinders collected specifically as archive samples to be stored, or used as working standards and not completely exhausted. Archive samples were screened for background conditions by examining trace gases such as CFC-12 as well as local wind direction at the time of sampling. Eight out of 68 potential archive samples were rejected based on concentrations of CFC-12, CFC-11, and/or wind direction not having been consistent with background air masses.

The integrated data set consists of both high-frequency in situ measurements and low frequency flask measurements. The uncertainty (standard error) for each month at each site was calculated using an effective number of independent measurements (N_{eff}). Although there are as many as 744 individual measurements per month at some sites, not all measurements are independent. We estimated the number of independent samples by calculating the time scale of auto correlation of hourly samples. Typically, hourly samples are auto-correlated ($\rho > 0.1$) for 12–48 h at a time at each site. This seems to correspond to the timescales of diurnal cycles or synoptic wave activity. Thus, we estimate that a monthly median estimate of SF_6 concentration consists of ∼15 independent estimates from in situ data and 3–4 independent estimates from flasks. Monthly standard deviations for each site were scaled by the square root of N_{eff}. The monthly uncertainty at each site was then determined as the mass-weighted mean standard error from each program (flasks and in situ) when data from both programs were available. An additional uncertainty was introduced when the mean mole fraction from each program differed by more than the combined standard errors. Hence, differences between two independent systems are incorporated as an additional term in the uncertainty. The mean difference between global mean SF_6 computed using flask and in situ data from 2000–2010 is < 0.01 ppt (see Fig. S3).

Monthly mean data were averaged in a mass-weighted (cosine latitude) fashion across seven latitude bins to produce global and hemispheric means. Uncertainty in the global mean was estimated by computing the global mean numerous times (Monte-Carlo method), randomly adjusting the monthly mean at each station within a 2-σ window (Normal distribution). Further, data gaps (up to 30 % of the data) were introduced at random to test the robustness of the gap-filling interpolation method. The integrated global mean data record shown in Fig. 7 was derived from 500 simulations. Global mean SF_6 from 1985–2005 can be approximated by the function $y = 0.125 \pm (0.012) + 0.215 \pm (0.001) \times (t–1985)$. This function supersedes that of Geller et al. (1997), and results from an updated SF_6 calibration scale, reanalysis

Table 3. Sampling sites.

Sampling site	Abbr.	Lat., Long.	Alt. (masl)	Obs.
Alert, Nunavut	ALT	82.5, −62.5	54	flask
Summit, Greenland	SUM	72.6, −38.5	3238	in situ
Barrow, AK	BRW	71.3, −156.6	30, 30	flask, in situ
Mace Head, Ireland	MHD	53.3, −9.9	25	flask
Trinidad Head, CA	THD	41.1, −124.2	107	flask
Niwot Ridge, CO	NWR	40.0, −105.5	3523, 3025	flask, in situ
Cape Kumukahi, HI	KUM	19.5, −154.8	3	flask
Mauna Loa, HI	MLO	19.5, −155.6	3397, 3397	flask, in situ
Cape Matatula, Am. Samoa	SMO	−14.2, −170.6	77, 77	flask, in situ
Cape Grim, Australia	CGO	−40.7, 144.7	94	flask
Palmer Station, Antarctica	PSA	−64.9, −64.0	10	flask
South Pole, Antarctica	SPO	−90.0, −24.8	2810, 2810	flask, in situ

of the archive samples analyzed by Geller et al. (1997), improved measurement precision, and a longer data record.

3.4 SF_6 growth rates

Global monthly mean SF_6 concentrations were used to derive global SF_6 growth rates by subtracting global monthly mean concentrations in successive years (e.g. January 2003–January 2002, February 2003–February 2002, etc.) (Fig. 8). Because SF_6 is extremely long-lived in the atmosphere, the increase in SF_6 concentration from one year to the next is essentially proportional to the emissions in that year. A close approximation of emissions in Gg yr^{-1} can be obtained by multiplying the growth rate (ppt yr^{-1}) by 25 (Maiss and Brenninkmeijer, 1998).

The average growth rate from 1986–2005, determined from NH archive samples was $0.214\,\text{ppt} \pm 0.001\,\text{yr}^{-1}$. In agreement with Levin et al. (2010) and Rigby et al. (2010), our results show that the global growth rate of SF_6 (emissions) increased gradually between 2001 and 2006, and rapidly from 2006-2008, reaching a peak of $0.30 \pm 0.03\,\text{ppt}\,\text{yr}^{-1}$ (or $\sim 7.4\,\text{Gg}\,\text{yr}^{-1}$ SF_6) in 2007–2008. SF_6 emissions increased at an average rate of $5\,\%\,\text{yr}^{-1}$ from 2001–2008. This corresponds to a period of rapid growth in world gross domestic product (GDP). The general features of global SF_6 growth rates since 1995 derived from these data are consistent with those of Levin et al. (2010) and Rigby et al. (2010).

Some inter-annual variability in SF_6 emissions is suggested from this simple analysis. Some of this apparent inter-annual variability is probably due to atmospheric transport (e.g. El-Niño Southern Oscillation, Quasi-biennial Oscillation) coupled with the distribution of measurement sites (Elkins et al., 1993). For example, only one station (SMO) lies in the tropical Southern Hemisphere, and air masses arriving at this site are influenced by large-scale climate variability (Hartley and Black, 1995; Patra et al., 2009). When SF_6 growth rates are examined on a site-by-site basis we observe some inter-annual variability that is consistent among most Northern Hemisphere sites (Fig. 9). Three features are notable in the recent decade: (a) a slight decline in the SF_6 growth rate in 2004, (b) an increase in the SF_6 growth rate from 2005–2008, (c) and a sharp decline in 2009. SF_6 growth rates at Mace Head, Ireland show larger variability, possible due to influence of large scale oscillations affecting atmospheric transport, such as the Arctic Oscillation and the North Atlantic Oscillation. Nevertheless, there is very good agreement among NH sites in 2008.

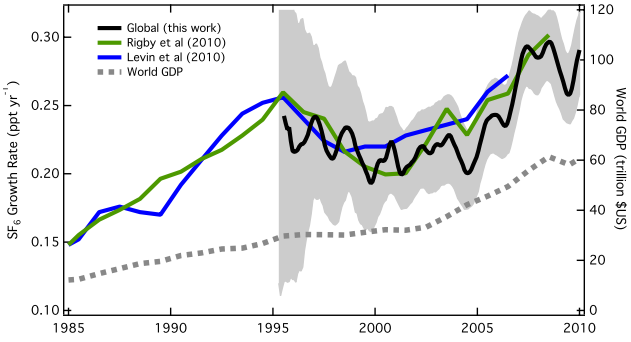

Fig. 8. Global growth rate (ppt yr^{-1}) determined from flask and in situ combined SF_6 dataset. (shaded region is 2-σ). Also shown are growth rates derived from emission estimated of Levin et al. 2010) and Rigby et al. (2010) along with World GDP (World Bank, 2011).

We estimate the effects of transport on the SF_6 growth rate by running the three-dimensional chemical transport model MOZART (Model for Ozone and Related Tracers, Emmons et al., 2010) with constant SF_6 emissions (from EDGAR version 4.0 for the year 2005) starting in the year 2000. The model was driven with NCEP/NCAR meteorological fields (Kalnay et al., 1996) to simulate the SF_6 mixing ratio at four NOAA/ESRL observing sites (BRW, MLO, SMO, SPO). We then compute global mean SF_6 and corresponding growth rates as before (Fig. 10b). Here, inter-annual variability

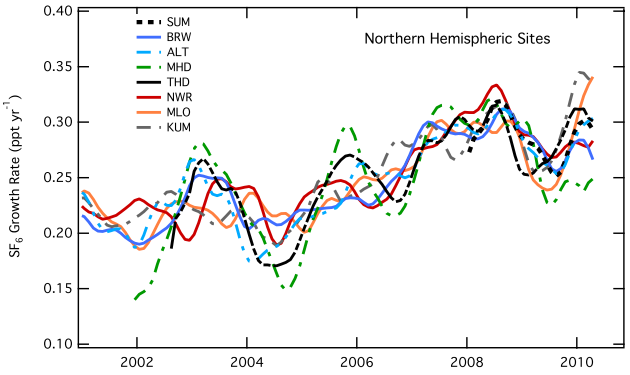

Fig. 9. SF_6 growth rates calculated on a site-by-site basis at eight NH sites.

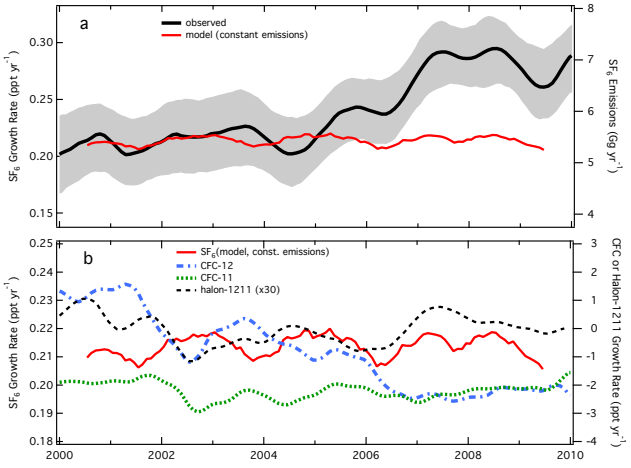

Fig. 10. (a) SF_6 growth rate derived from global mean SF_6 (shaded region is 2-σ), along with corresponding emissions (Gg yr^{-1}) calculated with a 2-box model (Geller et al., 1997) and with SF_6 growth rate derived from model results at four sites using constant SF_6 emissions (solid red) to assess transport-driven changes in the SF_6 growth rate; **(b)** observed growth rates of CFC-12 (blue), CFC-11 (green), halon-1211 (black, detrended) derived from global mean data, and model SF_6 repeated from **(a)**.

observed in the modeled SF_6 growth rate is due solely to transport. While not all features are consistent between the model and observations (Fig. 10a), three features in the later period of the data record stand out. The model suggests that the growth rate of SF_6 from 2005–2007 was modulated by transport, but that transport effects were small compared to changing emissions. The model does not support a decline in the SF_6 growth rate in 2004 as suggested by the data. Also, the double peak in SF_6 growth rate in 2007 and 2008 is transport-related, as is some of the decline in 2008–2009. These features are also present in growth rates of long-lived tracers CFC-11 and CFC-12, with global means and growth rates determined from NOAA/ESRL measurements (Table 3). The growth rates of CFC-11 and CFC-12 exhibit similar inter-annual variability (Fig. 10b) except during 2008–2009, during which no large transport-driven declines are observed.

The observed decline in the SF_6 growth rate from the peak in 2008 through mid-2009 is 14 %. From modeled SF_6 (constant emissions) and other long-lived tracers, we estimate that atmospheric transport is responsible for at most ∼30 % of the observed change. Therefore, the change in SF_6 emissions during 2008–2009 is estimated to be ∼10 %. This decline also coincides with a slowing of the world economy, with GDP decreasing ∼0.3 % following a decade of growth. Although such a rapid decline in emissions might seem unlikely, it is not unprecedented. Global SF_6 emissions declined 27 % from 1995 to 1998 (Maiss and Brenninkmeijer, 2000) and 8 % from 1996–1997 (Levin et al, 2010), and increased 8 % between 2006 and 2007. The decline in SF_6 emissions in 2008–2009 appears to be short-lived, as SF_6 growth rates began to increase in early 2010, approaching their peak value observed in 2008.

4 Conclusions

By modifying a common GC technique used to measure N_2O and SF_6, we have improved the precision of SF_6 measurement by a factor of 2–3. The precision associated with a calibration instrument, used to transfer the NOAA-2006 scale to tertiary compressed gas standards, has been improved in recent years and is currently around 0.3 % or ∼0.02 ppt based on ambient SF_6 levels. As this technique is extended to instruments currently in use, our ability to quantify SF_6 emissions on global and regional scales should improve. While good SF_6 precision has been demonstrated using two columns and P-5 carrier gas, the system described here may be most useful when high-quality P-5 is difficult to obtain.

Mixing ratios of SF_6, measured in flasks collected at 12 sites around the world, and measured in situ at six sites, continue to increase in the troposphere. The growth rate (and inferred emissions of SF_6) has increased in recent years reaching a maximum of 0.30 ±0.03 ppt yr^{-1}. This is almost 40 % larger than the average growth rate of 0.21 ppt yr^{-1} deduced from archive samples in the NH collected between 1987 and 2005. When SF_6 growth rates are examined on a station-by-station basis, all NH sites show two similar features: an increase in the growth rate from 2005–2008, and a decrease in the growth rate from 2008 through mid-2009. The increase in SF_6 growth rate corresponds to an increase in World GDP through 2008, while the recent slowing of SF_6 growth rate corresponds to a decline in world economic growth. The short-lived decline in SF_6 emissions observed during 2008–2009 is estimated to be about 10 % of the 2008 maximum.

Supplementary material related to this article is available online at: http://www.atmos-meas-tech.net/4/2441/2011/amt-4-2441-2011-supplement.pdf.

Acknowledgements. We are indebted to station personnel for steadfast flask collection and operation of in situ systems. We appreciate the discussions and assistance provided by Andrew Crotwell, Andy Clarke, Gabrielle Petron, and Ron Prinn. This work was supported, in part, through NOAA's Atmospheric Composition and Climate Program, and Office of Oceanic and Atmospheric Research's Climate Program Office. MR is supported through the Advanced Global Atmospheric Gases Experiment (AGAGE), by NASA Upper Atmospheric Research Program grants NNX07AE89G and NNX11AF17G to MIT.

Edited by: M. von Hobe

References

Bakwin, P. S., Hurst, D. F., Tans, P. P., and Elkins, J. W.: Anthropogenic sources of halocarbons, sulfur hexafluoride, carbon monoxide, and methane in the southeastern United States, J. Geophys. Res, 102, 15915–15925, 1997.

Elkins, J. W.: Determination of dissolved nitrous oxide in aquatic systems by gas chromatography using electron-capture detection and multiple phase equilibration, Anal. Chem., 52, 263–267, 1980.

Elkins, J. W. and Dutton, G. S.: Nitrous oxide and sulfur hexafluoride, in State of the Climate in 2008, B. Am. Meteor. Soc., 90, 1–196, 2009.

Elkins, J. W., Thompson, T. M., Swanson,T. H., Butler, J. H., Hall, B. D., Cummings, S. O., Fisher, D. A., and Raffo, A. G.: Decrease in the growth rates of atmospheric chlorofluorocarbons 11 and 12, Nature, 364, 780–783, 1993.

Elkins, J. W., Fahey, D. W., Gilligan, J. M., Dutton, G. S., Baring, T. J., Volk, C. M., Dunn, R. E., Myers, R. C., Montzka, S. A., Wamsley, P .R., Hayden, A. H., Butler, J. H., Thompson, T. M., Swanson, T. H., Dlugokencky, E. J., Novelli, P. C., Hurst, D. F., Lobert, J. M., Ciciora, S. J., McLaughlin, R. J., Thompson, T. L., Winkler, R. H., Fraser, P. J., Steele, L. P., Lucarelli, M. P.: Air-borne gas chromatograph for in situ measurements of long-lived species in the upper troposphere and lower stratosphere, Geophys. Res. Lett., 23, 347–350, 1996.

Emmons, L. K., Walters, S., Hess, P. G., Lamarque, J.-F., Pfister, G. G., Fillmore, D., Granier, C., Guenther, A., Kinnison, D., Laepple, T., Orlando, J., Tie, X., Tyndall, G., Wiedinmyer, C., Baughcum, S. L., and Kloster, S.: Description and evaluation of the Model for Ozone and Related chemical Tracers, version 4 (MOZART-4), Geosci. Model Dev., 3, 43–67, doi:10.5194/gmd-3-43-2010, 2010.

Engel, A., Möbius, T., Bönisch, H., Schmidt, U., Heinz, R., Levin, I., Atlas, E., Aoki, S., Nakazawa, T., Sugawara, S., Moore, F., Hurst, D., Elkins, J., Schauffler, S., Andrews, A., and Boering, K., Age of stratospheric air unchanged within uncertainties over the past 30 yr. Nat. Geosci., 2, 28–31, doi:10.1038/ngeo388, 2009.

Fehsenfeld, F. C., Goldan, P. D., Phillips, M. P., and Sievers, R. E.: Selective electron-capture sensitization, in Electron Capture: Theory and Practice in Chromatography, edited by: Zlatkis, A. and Poole, C. F., Journal of Chromatography Library, 20, 429, Elsevier, New York, 1981.

Forster, P., Ramaswamy, V., Artaxo, P., Berntsen, T., Betts, R., Fahey, D. W., Haywood, J., Lean, J., Lowe, D. C., Myhre, G., Nganga, J., Prinn, R., Raga, G., Schulz, M., and Van Dorland, R.: Changes in Atmospheric Constituents and in Radiative Forcing, in: Climate Change 2007, The Physical Science Basis, Contribution of Working Group I to the Fourth Assessment Report of the Intergovernmental Panel on Climate Change, edited by: Solomon, S., Qin, D., Manning, M., Chen, Z., Marquis, M., K., Averyt, B., Tignor, M., and Miller, H. L., Cambridge University Press, Cambridge, United Kingdom and New York, 2007.

Geller, L., Elkins, J. W., Lobert, J., Clarke, A., Hurst, D. F., Butler, J., and Myers, R., Tropospheric SF_6: Observed latitudinal distribution and trends, derived emissions and inter-hemispheric exchange time, Geophys. Res. Lett., 24, 675–678, 1997.

Gloor, M., Dlugokencky, E., Brenninkmeijer, C., Horowitz, L., Hurst, D. F., Dutton, G., Crevoisier, C., Machida, T., and Tans, P.: Three-dimensional SF_6 data and tropospheric transport simulations: Signals, modeling accuracy, and implications for inverse modeling, J. Geophys. Res., 112, D15112, doi:10.1029/2006JD007973, 2007.

Hall, B. D., Dutton, G. S., and Elkins, J. W.: The NOAA nitrous oxide standard scale for atmospheric observations, J. Geophys. Res., 112, D09305, doi:10.1029/2006JD007954, 2007.

Hall, B. D., Engel, A., Mühle, J., Elkins, J. W., Atlas, E., Blake, D., Weiss, R., Vollmer, M., Rhoderick, J., Fraser, P., Brunke, E., Worthy, D., Artuso, F., Levin, I., Maione, M., Scheel, H. E., O'Doherty, S., Reimann, S., Yokuchi, Y., Saltzman, E., Happell, J., Loewenstein, M., and Chiavarini, S.: Results from the International Halocarbons-In-Air Comparison Experiment, Atm. Meas. Tech., in preparation, 2011

Harnisch J. and R. Gluckman: European Climate Change Programme, Working Group Industry, Work Item Fluorinated Gases, Brussels, 2001.

Hartley, D. E. and Black, R. X., Mechanistic analysis of interhemispheric transport, Geophys. Res. Lett., 22, 2945–2948, 1995.

Hurst, D. F., Lin, J. C., Romashkin, P. A., Daube, B. C., Gerbig, C., Matross, D. M., Wofsy, S. C., Hall, B. D., and Elkins, J. W.: Continuing global significance of emissions of Montreal Protocol–restricted halocarbons in the United States and Canada, J. Geophys. Res., 111, D15302, doi:10.1029/2005JD006785, 2006.

Kalnay, E., Kanamitsu, M., Kistler, R., Collins, W., Deaven, D., Gandin, L., Iredell, M., Saha, S., White, G.,Woollen, J., Zhu, Y., Chelliah, M., Ebisuzaki, W., Higgins, W., Janowiak, J., Mo, K., Ropelewski, C., Wang, J., Leetmaa, A., Reynolds, R., Jenne, R., and Joseph, D.: The NCEP/NCAR 40 yr reanalysis project, B. Am. Meteorol. Soc., 77, 437–471, 1996.

Levin, I. and Hesshaimer, V., Refining of atmospheric transport model entries by the globally observed passive tracer distributions of ^{85}krypton and sulfur hexafluoride (SF_6), J. Geophys. Res., 101, 16745–16756, 1996.

Levin, I., Naegler, T., Heinz, R., Osusko, D., Cuevas, E., Engel, A., Ilmberger, J., Langenfelds, R. L., Neininger, B., Rohden, C. v.,

Steele, L. P., Weller, R., Worthy, D. E., and Zimov, S. A.: The global SF6 source inferred from long-term high precision atmospheric measurements and its comparison with emission inventories, Atmos. Chem. Phys., 10, 2655–2662, doi:10.5194/acp-10-2655-2010, 2010.

Maiss, M. and Brenninkmeijer, C. A. M.: Atmospheric SF_6: trends, sources, and prospects, Environ. Sci. Technol., 32, 3077–3086, 1998.

Maiss, M. and Brenninkmeijer, C.: A reversed trend in emissions of SF_6 into the atmosphere?, in: Non-CO_2 Greenhouse Gases: Scientific Understanding, edited by: van Ham, J., Baede, A. P. M., Meyer, L. A., and Ybema, R., Proceedings of the Second International Symposium, Noordwijkerhout, The Netherlands, 8–10 September 1999, Kluwer Academic Publishers, Dordrecht, Netherlands, 2000.

Miller, B. R., Weiss, R. F., Salameh, P. K., Tanhua, T., Greally, B. R., Muhle, J., and Simmonds P. G.: Medusa: A sample preconcentration and GC/MS system for in situ measurements of atmospheric trace halocarbons, hydrocarbons, and sulfur compounds, Anal. Chem., 80, 1536–1545 doi:10.1021/ac702084k, 2008.

Moore, F. L., Elkins, J. W., Ray, E. A., Dutton, G. S., Dunn, R. E., Fahey, D. W., McLaughlin, R. J., Thompson, T. L., Romashkin, P. A., Hurst, D. F., and Wamsley, P. R.: Balloonborne in situ gas chromatograph for measurements in the troposphere and stratosphere, J. Geophys. Res., 108, 8330, doi:10.1029/2001JD000891, 2003.

Morris, R. A., Miller, T. M., Viggiano, A. A., Paulson, J. F., Solomon, S., and Reid, G.: Effects of electron and ion reactions on atmospheric lifetimes of fully fluorinated compounds, J. Geophys. Res., 100, 1287–1294, 1995.

Park, J. H., Ko, M. K. W., Jackman, C. H., Plumb, R. A., Kaye, J. A., and Sage, K. H.: Models and Measurements Intercomparisons II, NASA Technical Memorandum 1999-209554, 494 pp., 1999.

Patra, P. K., Takigawa, M., Dutton, G. S., Uhse, K., Ishijima, K., Lintner, B. R., Miyazaki, K., and Elkins, J. W.: Transport mechanisms for synoptic, seasonal and interannual SF_6 variations and "age" of air in troposphere, Atmos. Chem. Phys., 9, 1209–1225, doi:10.5194/acp-9-1209-2009, 2009.

Ravishankara, A. R., Solomon, S., Turnipseed, A. A., and Warren, R. F.: Atmospheric lifetimes of long-lived halogenated species, Science, 259, 194–199, 1993.

Ray, E. A., Moore, F. L., Rosenlof, K. H., Davis, S. M., Boenisch, H., Morgenstern, O., Smale, D., Rozanov, E., Hegglin, M., Pitari, G., Mancini, E., Braesicke, P., Butchart, N., Hardiman, S., Li, F., Shibata, K., and Plummer, D. A.: Evidence for changes in stratospheric transport and mixing over the past three decades based on multiple data sets and tropical leaky pipe analysis, J. Geophys. Res., 115, D21304, doi:10.1029/2010JD014206, 2010.

Rigby, M., Mühle, J., Miller, B. R., Prinn, R. G., Krummel, P. B., Steele, L. P., Fraser, P. J., Salameh, P. K., Harth, C. M., Weiss, R. F., Greally, B. R., O'Doherty, S., Simmonds, P. G., Vollmer, M. K., Reimann, S., Kim, J., Kim, K.-R., Wang, H. J., Olivier, J. G. J., Dlugokencky, E. J., Dutton, G. S., Hall, B. D., and Elkins, J. W.: History of atmospheric SF_6 from 1973 to 2008, Atmos. Chem. Phys., 10, 10305–10320, doi:10.5194/acp-10-10305-2010, 2010.

Simmonds, P. G., Shoemake, G. R., Lord, H. C., and Lovelock, J. E.: Improvements in the determination of sulfur hexafluoride for use as a meteorological tracer, Anal. Chem., 44, 860–863 1972.

Thompson, R. L., Manning, A. C., Gloor, E., Schultz, U., Seifert, T., Hänsel, F., Jordan, A., and Heimann, M.: In-situ measurements of oxygen, carbon monoxide and greenhouse gases from Ochsenkopf tall tower in Germany, Atmos. Meas. Tech., 2, 573–591, doi:10.5194/amt-2-573-2009, 2009.

UNFCCC: United Nations Framework Convention on Climate Change, National Inventory Submissions, 2010.

US EPA: SF_6 emission reduction partnership for electric power systems, Annual Report, EPA 430R08039, 2008.

van der Laan, S., Neubert, R. E. M., and Meijer, H. A. J.: A single gas chromatograph for accurate atmospheric mixing ratio measurements of CO_2, CH_4, N_2O, SF_6 and CO, Atmos. Meas. Tech., 2, 549–559, doi:10.5194/amt-2-549-2009, 2009.

Wanninkhof, R., Watson, A. J., and Ledwell, J. R.: Analysis of sulfur hexafluoride in seawater, J. Geophys. Res., 95, 9733–8740, 1991.

World Bank, http://data.worldbank.org/indicator/NY.GDP.MKTP.CD, Last Date of Access: 20 April 2011.

Worthy, D. E., Platt, J. A., Kessler, R., Ernst, M., and Racki, S.: The Greenhouse Gases Measurement Program, Measurement Procedures and Data Quality, Meteorological Service of Canada, 97–120, 2003.